PHILOSOPHICAL TRANSACTIONS OF THE ROYAL SOCIETY B BIOLOGICAL SCIENCES

# Dynamics of Arthropod Filiform Hairs. III. Flow Patterns Related to Air Movement Detection in a Spider (Cupiennius salei KEYS.)

Friedrich G. Barth, Joseph A. C. Humphrey, Ute Wastl, Johannes Halbritter and Waltraud Brittinger

*Phil. Trans. R. Soc. Lond. B* 1995 **347**, 397-412
doi: 10.1098/rstb.1995.0032

# Dynamics of arthropod filiform hairs. III. Flow patterns related to air movement detection in a spider (*Cupiennius salei* KEYS.)

FRIEDRICH G. BARTH[1]*, JOSEPH A. C. HUMPHREY[2], UTE WASTL[1], JOHANNES HALBRITTER[1] AND WALTRAUD BRITTINGER[1]

[1] *Biozentrum, Institut für Zoologie, Universität Wien, Althanstraße 14, A-1090 Wien, Austria*
[2] *Department of Mechanical Engineering, University of California at Berkeley, Berkeley, California 94720, U.S.A.*

## CONTENTS

| | PAGE |
|---|---|
| 1. Introduction | 398 |
| 2. Materials and methods | 398 |
| (*a*) Sensory space | 398 |
| (*b*) Air flow around the spider | 399 |
| (*c*) Field measurements | 400 |
| 3. Results | 401 |
| (*a*) Sensory space | 401 |
| (*b*) Undisturbed air flow around the spider in the wind tunnel | 402 |
| (*c*) Air flow due to the fly | 406 |
| (*d*) Background noise in the field | 409 |
| 4. Discussion | 409 |
| (*a*) Range of the trichobothria | 409 |
| (*b*) Undisturbed air flow around the spider | 410 |
| (*c*) Prey signals | 410 |
| References | 411 |

## SUMMARY

In previous studies we related the mechanical properties of spider trichobothria to a generalized mathematical model of the movement of hair and air in filiform medium displacement receivers. We now present experiments aimed at understanding the complex stimulus fields the trichobothrial system is exposed to under natural conditions.

Using the elicitation of prey capture as an indicator and a tethered humming fly as a stimulus source, it has been shown that the behaviourally effective range of the trichobothrial system in *Cupiennius salei* Keys. is approximately 20 cm in all horizontal directions. Additionally, the fly still elicits a suprathreshold deflection of trichobothria while distanced 50–70 cm from the spider prosoma.

To gain insight into the fluid mechanics of the behaviourally effective situation we studied: first, undisturbed flow around the spider in a wind tunnel; second, background flow the spider is exposed to in the field; and third, flow produced by the tethered flying fly.

1. The motion of air around a complex geometrical structure like a spider is characterized by an uneven distribution of flow velocities over the spider body. With the flow approaching from the front, both the mean and r.m.s. values are higher above the legs than above the pro- and opisthosoma; the velocity in the wake behind the spider, however, is markedly decreased. The pattern of these gradients is more complicated when the spider's horizontal orientation is changed with respect to the main flow direction. It introduces asymmetries, for exmple, increased vortical, unsteady flow on the leeward compared with the windward side.

2. Sitting on its dwelling plant and ambushing prey in its natural habitat, the background air flow around *Cupiennius* is characterized by low frequencies ($< 10$ Hz), a narrow frequency spectrum, and low velocities (typically below 0.1 m $s^{-1}$ with less than 15% r.m.s. fluctuation).

3. The distinctive features of a biologically significant air flow (for example, that produced by the humming fly) seem to be a concentrated, i.e. directional unsteady, high speed flow of the order of 1 m $s^{-1}$, and a relatively broad frequency spectrum containing frequencies much higher than those of the

* To whom correspondence should be sent.

background flow. For a spider, sitting on a solid substrate (a leaf of a bromeliad, for example), air speed just above the substrate increases and thus provides higher sensitivity when compared to a spider in a orb web, which is largely transparent to the airflow. The flow patterns stimulating the ensemble of the trichobothria contain directional cues in both the undisturbed flow and the flow due to prey cases.

## 1. INTRODUCTION

For many arthropods, patterns of air flow are an important source of information. Included in this group are orthopterans such as crickets (Tobias & Murphey 1979; Dambach *et al.* 1983; Dambach & Heinzel 1985) and cockroaches (Roeder 1963; Camhi 1980; Stierle *et al.* 1994), caterpillars (Tautz 1977; Tautz & Markl 1978), scorpions (Hoffmann 1967; Linsenmaier 1968), and spiders (Hergenröder & Barth 1983*a*,*b*; Reißland & Görner 1985). The sensory devices picking up air flow signals, and guiding behavioural responses such as prey capture and defensive behaviour, are the filiform hairs or thread-hairs. In spiders these hairs are called trichobothria. Physically, trichobothria (like other filiform hairs) are classified as displacement receivers, deflected by viscous forces when exposed to the slightest movement of air (Barth *et al.* 1993; Humphrey *et al.* 1993).

Recent years have seen substantial progress in our understanding of the physics behind the working of individual thread hairs. One major advance was to attain an appreciation as to the significance of the boundary layer, which develops above the cuticular surface in the presence of air flow and whose thickness is related to the mechanical frequency tuning shown by a hair of a particular length (Tautz 1979; Shimozawa & Kanou 1984; Barth *et al.* 1993; Humphrey *et al.* 1993).

To date, the central nervous representation of orthopteran cercal hairs has been particularly well studied (for a review, see Boyan & Ball 1990), however, very little is known about natural stimulus fields and their relation to the morphological and functional properties of arthropod wind-sensitive sensory systems. The distinctive features of biologically significant and insignificant air flows have barely been examined. The available data mainly refer to insect escape behaviour (Camhi & Tom 1978; Camhi *et al.* 1978; Tautz & Markl 1978; Reißland & Görner 1985; Gnatzy & Kämper 1990).

It is these same aspects in a large ctenid wandering spider (*Cupiennius salei* Keys.) that we study here. This spider has an air movement detecting system consisting of nearly 1000 trichobothria, widely distributed over the legs and pedipalps and forming specific patterns of arrangement and length distribution. Of all the spiders studied so far, *Cupiennius salei* has the largest number of trichobothria by far, suggesting a particular behavioural significance of air movement detection in this species (Peters & Pfreundt 1986; Barth *et al.* 1993). The two previous studies in this series reported many of the morphological and mechanical properties of *Cupiennius* trichobothria and related them to a mathematical model of the hair and air motions (Barth *et al.* 1993; Humphrey *et al.* 1993). The current study seeks to provide some understanding of the stimulus mechanism, on a larger scale. It provides data on the spatial range of the trichobothrial system, and on the undisturbed air flow past the spider and her dwelling plant, under lab and field conditions. We also describe an air movement signal induced by a fly, promptly releasing prey capture behaviour. The bulk of the existing literature on insect flight deals with forces on the wings and the work and power produced (see for example, Nachtigall 1973; Weis-Fogh 1973; Maxworthy 1981; Ellington 1984). The insect wing motions, including those of dipteran insects, are complex and lead to a highly unsteady, vortical state of the air motion around and downstream of an insect. In this investigation we are concerned with the motion of air downstream of a fly, which is of little interest to the aerodynamics of insect flight.

In view of the complexity of the subject in hand, we consider this study to be a humble beginning which aims toward a first understanding of what may be important, rather than a quantitative explanation of a wealth of details.

## 2. MATERIALS AND METHODS

### (*a*) *Sensory space*

#### (i) *Behaviour*

*Cupiennius salei* (Ctenidae) was used in all experiments (Lachmuth *et al.* 1984), a Central American hunting spider (Barth *et al.* 1988) bred and raised in the Vienna Zoological Institute. Young spiders 6–7 months old, still approximately four months away from adulthood, were used to study behavioural responses to an air movement signal produced by a tethered but flying fly. The readiness of the spider to respond to prey stimuli is higher at this age than in adults, and can be kept high by adhering to a strict feeding schedule, providing only two flies, twice a week.

The flies used to provide the air flow representing a prey signal were *Sarcophaga carnaria*. To attach the fly to the lower end of a thin wooden rod, a small piece of paper was glued dorsally to the thorax. Upon removal of a small piece of paper held between it's legs by tarsal contact, the fly began stationary flight. The long axis of the fly was always kept horizontal with the abdomen pointing towards the spider prosoma. To determine the $x$, $y$, and $z$ coordinates of the fly relative to the spider, the experimental arena was covered with grid paper, a mirror was used to give the side view of the fly alongside a ruler, and all experiments were videotaped from above.

The spider was free to move during experiments, it's response to the fly signal was counted positive if it moved quickly towards the fly as it does only during actual prey capture. (Occasional, spurious leg movements noted in otherwise stationary spiders were not rated as a responses.) Neither vision or olfaction were involved in eliciting response to the fly signal; the




PHILOSOPHICAL TRANSACTIONS OF THE ROYAL SOCIETY B BIOLOGICAL SCIENCES

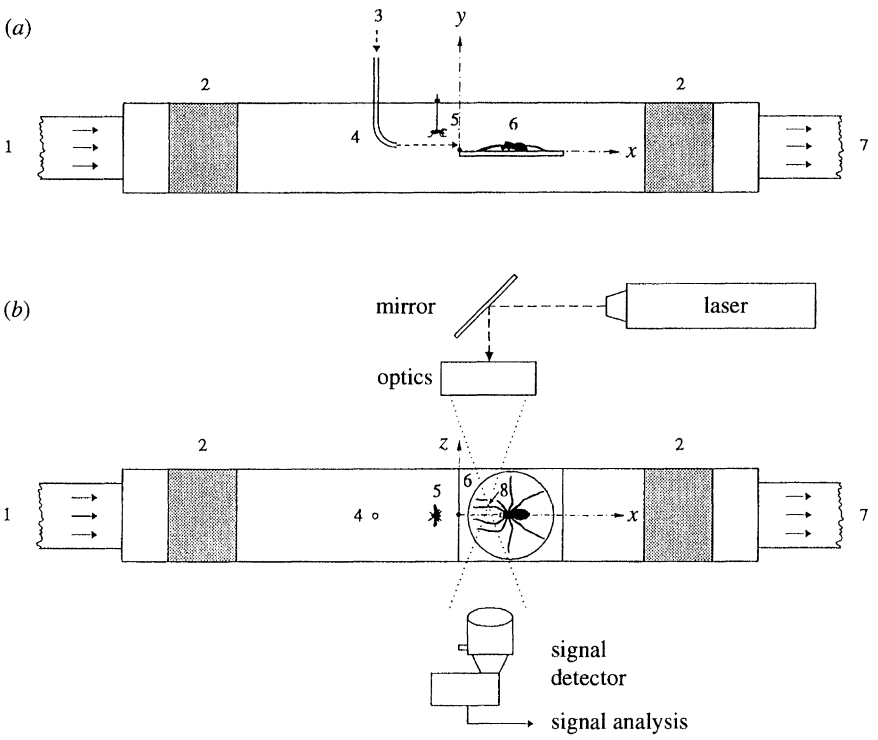


Figure 1. Test section for the analysis of air flow in a wind tunnel of square cross section ($10 \times 10$ cm$^2$): schematic representation of experimental arrangement. 1 = entry to duct; 2 = hexagonal mesh honey comb (diameter 0.5 cm, length 7.5 cm); 3 = incense smoke for flow visualization; 4 = smoke rake; 5 = fly tethered to hypodermic tube; 6 = platform with spider; 7 = exit of duct; 8 = optical probe volume defined by the crossing of two laser beams.

response continued when the eyes were covered (Hergenröder & Barth 1983*b*) and when working in red light (Barth *et al.* 1993). A response was also produced by arteficial air currents, but disappeared after ablation of all trichobothria.

(ii) *Deflection of trichobothria*

Adult females of *Cupiennius salei* were mounted on a spider holder with thin jointed metal legs, which allowed us to position their legs naturally, using sticky tape. (Barth & Geethabali 1982). This holder was then mounted on top of the vertical axis around which the fly could be rotated. The flies were mounted on a rod and stationary flight was induced as described above. Again, the long axis of the fly always remained horizontal with the abdomen pointing towards the spider. The direction taken by the first right leg of the spider was defined as an azimuth of 0°. The inclination angle $\alpha$ of the fly's position relative to the spider prosoma (see figure 2) was 10°, 30°, or 50° and the distance between fly (thorax) and spider (prosoma) either 8 cm or 12 cm, in experiments in which the angular position of the fly was changed. This distance measured up to 50 cm in experiments designed to record the largest distance of the fly at which the trichobothria were still deflected. To imitate the effect of a solid substrate such as the dwelling plant, the spider was mounted onto a solid plexiglass disk 26 cm in diameter, with no empty spaces between the legs, as with the spider holder.

Trichobothrial deflection (peak to peak excursion of tip) was measured under dark field illumination on the first leg (R1) with a binocular microscope (magnification $\times 50$; calibrated ocular grid; working distance 9.2 cm, resolution 2.5–5.0 μm) and the deflection angle determined as described in detail earlier (Barth *et al.* 1993).

### (*b*) *Air flow around the spider*

(i) *Experimental apparatus*

The experimental wind tunnel apparatus was a closed-loop air flow system composed of a transparent test section, where the visualization and laser-Doppler velocimeter (LDV) measurements were made, and a corrugated flexible tube for the return flow. The test section (see figure 1) was a straight duct of square ($10 \times 10$ cm$^2$) cross section constructed from 1 cm thick plexiglass. A fixed speed electric fan connected to the tube provided the necessary air mass flow which was stably controlled to within $\pm 1$ % of the bulk average velocity, using a variable diameter orifice. Both the fan and the orifice were placed downstream of the test section to minimize any possible disturbances to the flow passing through the test section. The orifice settings were calibrated with the LDV. In the test section itself, two pieces of hexagonal mesh honeycomb were fitted near the entry and exit planes to the duct. LDV measurements confirmed a uniform and steady (non-turbulent) air flow.

The spider platform, spanning the 10 cm width of the duct, was 2 mm thick and 11.5 cm long with its leading edge located 24.5 cm (2.45 duct diameters) downstream of the inlet flow honeycomb section. The platform could be tilted either downwards or upwards and allowed 360 ° rotation of a circular section (8.5 cm in diameter) positioned at its centre. In this way, it was possible to set the spider at any orientation with respect to the approaching flow. A lid on the duct provided

quick access to the interior. For flow visualization, incense smoke (cooled to room temperature) was introduced through the lid in the form of a smoke rake, by seven equidistantly spaced stainless steel, 1 mm diameter tubes. The rake was located 9.5 cm upstream of the platform with a variable penetration depth. The tips of the tubes were curved in the direction of the air flow to minimize disturbances to the air stream. For the conditions investigated, the maximum Reynolds number of a smoke tube never exceeded 42, the approximate critical value required for the onset of flow unsteadiness past a cylinder in free flow.

An additional hole, 2.5 cm upstream of the platform, allowed the insertion of a straight, 1 mm diameter hypodermic tube from which to tether a fly. Another hole allowed the insertion of a rotatable mount, supporting a small ball of paper which could be placed (or removed from) under the fly. Interruption of fly tarsal contact with this ball initiated flight. When removed, the ball of paper and its tube support were both out of the flow path, and no longer sources of possible perturbations; the penetration depths of both tubes were also variable.

(ii) *Measurement techniques*

Still photographs and video recordings were made of the visualized flow field for conditions involving: a fly alone, with and without the platform present; a spider alone; and a spider in the presence of a tethered fly (altering the background flow by flapping its wings). The visualization experiments were qualitative in nature but provided a wealth of information concerning the spatial and temporal characteristics of the respective flows. In particular, visualization was critical for revealing the extent to which the background flow was perturbed by the spider and/or the fly, a task which would have been extremely laborious to undertake via LDV point measurements of velocity alone.

Quantitative point measurements of the mean and r.m.s. streamwise component of velocity were also made for specific cases of fly alone and spider alone configurations. For this, one of the channels of a two-colour DANTEC 55X modular optics LDV unit coupled to a 5 watt argon-ion laser was used in backscatter mode; for details see Treidler (1991). The optical probe volume had the following approximate $e^{-2}$ dimensions: 0.1 mm × 0.1 mm × 1.0 mm, and could be traversed inside the duct. The fringe spacing in the probe volume was approximately 3 $\mu$m; after spatial filtering there were approximately 30 fringes within it. The relative r.m.s. (%) is defined as the r.m.s. velocity divided by the local flow velocity multipied by a factor of 100.

For the LDV measurements the duct flow was periodically seeded with silicone oil particles 0.1–10 $\mu$m in diameter. Typically, validated Doppler burst data rates betweeen 20–300 Hz could be obtained. The mean and r.m.s. values of velocity were based on 1000 individual realizations of velocity for the measurements made in the absence of a tethered fly, and on 4000 realizations made in the presence of a fly. The higher number of realizations made in the presence of a fly was due to the larger variations in velocity, induced by the motions of the wings. Coordinate locations will be referred to according to $(x, y, z)$ where, with reference to figure 1, the origin of coordinates is located at the centre of the leading edge of the platform, $x$ is aligned in the longitudinal or main flow direction, $y$ is aligned in the vertical direction, and $z$ is aligned in the spanwise direction (the $z = 0$ position, therefore, denotes the geometrical symmetry plane in the top view of the duct). Thus, for example, $(30, 0, -10)$ refers to a coordinate location with $x = 30$ mm, $y = 0$ mm and $z = -10$ mm. Similarly, a velocity profile measured along the $y$ coordinate direction with $x = 30$ mm and $z = -10$ mm is referred to as the $(30, y, -10)$ profile. Parts of the flow field around the spider were optically inaccessible as a result of the spider's body or legs blocking the LDV laser beams.

(iii) *Uncertainties*

The main sources of uncertainty affecting the mean and r.m.s. measurements of velocity were velocity gradient broadening, flow unsteadiness and finite size of the data sample. Additional possible sources of uncertainty were the optical probe volume location and orientation, the half angle between the laser beams, incomplete signal bias, filter bias, and velocity bias, but these were minimized. Treidler (1991) discusses these uncertainties. Their cumulative effect on the present measurements has been to introduce systematic and random errors of approximately 0.2 % and 1.0 % respectively, in the mean velocity measurements, and of approximately 5 % and 3 % in the r.m.s.

### (*c*) *Field measurements*

Air flow was measured above spiders in their natural habitat in Costa Rica (Wilson Botanical Garden, OTS-station, Las Cruces, Coto Brus). The species studied was *Cupiennius coccineus* which is very similar to *Cupiennius salei* with regard to aspects under examination in this study (Barth *et al.* 1988). Air flow was measured on ten consecutive days (in February 1992), above 22 different spiders sitting on 22 different individual plants (bromeliads and banana plants). A battery driven hot wire anemometer allowed the measurement of air flow velocities down to 0.5 cm $s^{-1}$ (design: Szpetkowski and Machan). Two parallel wires were used to extend the dynamic range of the probe (design: Institute of Geomechanics of the Polish Academy of Sciences, Krakow). The high temperature of the hot wire guaranteed virtual independence from ambient air temperature. The electronic circuit was designed to allow a large range of wind velocities between close to 0 cm $s^{-1}$ and 400 cm $s^{-1}$. For such a large working range, the display of the measured values which are available both as analogue signals and as proportional frequencies had to be partially linearized. A modified DAT-recorder (Sony DT-120) with a lower limit below 0.2 Hz (lowest frequency tested) served to record the frequency modulated (FM) output of the anemometer. The FM signal was converted into an analogue signal using a frequency demodulator and the analogue signal was then analysed using a CED 1401 (Cambridge Electronic Devices; spike 2).




PHILOSOPHICAL TRANSACTIONS OF THE ROYAL SOCIETY B BIOLOGICAL SCIENCES

The data were sampled at 100 Hz (duration of sampled record 10 s, resolution of fast Fourier transform (FFT) 0.1 Hz) and at 200 Hz (5 s, resolution of FFT 0.2 Hz). From the data recorded, a 51.2 s period was selected for FFT-analysis (1024 points). The same sample was then divided up into five periods of 10.24 s, and again these were subjected to FFT-analyses to produce higher temporal resolution.

Air movement was measured approximately 1 cm above the spider's prosoma with the most sensitive axis of the transducer oriented in the *x*, *y*, and *z* directions, relative to a plane parallel to the plant the spider was sitting on. Wind velocities are given as mean values together with the degree of fluctuation. Typically, only very low frequencies below 2 Hz are contained in the spectra. Fluctuation was, therefore, also calculated for the most relevant frequency range between 0.8 and 1.6 Hz.

## 3. RESULTS

### (*a*) *Sensory space*

#### (i) *Behaviour*

We have known for a long time that air movement such as that produced by a fly in flight can elicit prey capture behaviour in *Cupiennius* effectively (Hergenröder & Barth 1983*a*,*b*). Before setting out to study any details of the air flow around a spider, however, we strived for a more precise idea of the spatial working range of the sense detecting air movement and its behavioural significance. Reports on the behaviour of web spiders (Görner & Andrews 1969) have underlined the importance of clarifying this issue. These spiders (Agelenidae) only showed prey capture behaviour if the source of air movement was less than approximately 1 cm away (Görner & Andrews 1969). Casual observation of *Cupiennius* had indicated a considerably larger range which would entail far reaching consequences for the interpretation of natural air flows past the spider (see Discussion).

Our experiments on the limits of the sensory space (see figure 2*a*) showed that oriented locomotor behaviour towards a fly in stationary flight could be elicited from a spatial distance of up to approximately 27 cm, provided the fly's abdomen (always horizontally oriented) pointed towards the spider. The angle $\alpha$ (see figure 2*a*) formed by the fly, the spider prosoma and the platform therefore varied from almost 0° to 90° and still elicited a response. Correspondingly, the effective air movement signal emitted by the fly has a considerable extension along the plane including the fly's long axis and stretching perpendicularly down to the substrate. Some spiders respond rarely or not at all to stimulation from behind. When pooling the data from all animals examined, however, the response frequencies did not differ significantly from each other when the fly's position changed all around the spider (with the long axis of the fly always oriented parallel to one eight spider legs).

According to another set of experiments, where the vertical distance of the fly from the platform was kept consistently close to 5 cm and 10 cm, respectively, the highest percentages of responses by the spider to the fly signal were found 7–12 cm away (see figure 2*b*).

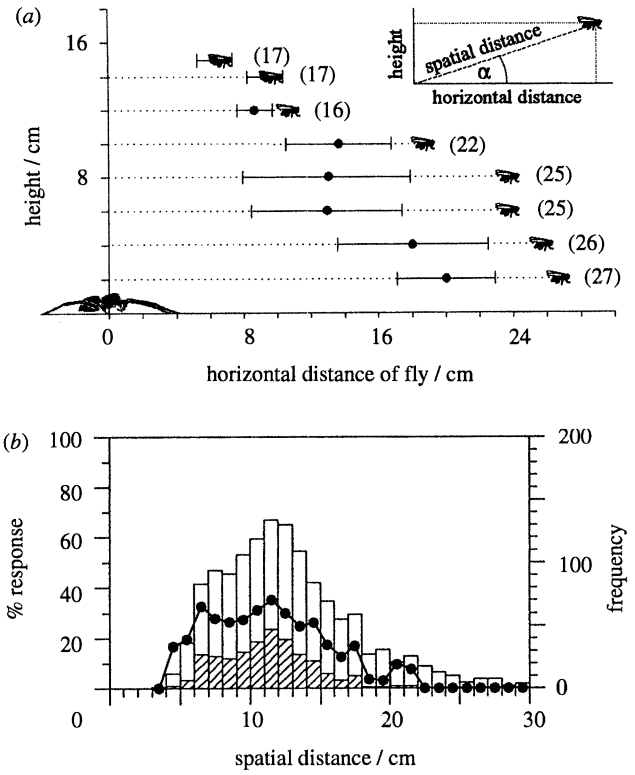


Figure 2. Behavioural response of spider to the air movement signal emitted by a tethered flying fly. (*a*) Maximum distance (average ± s.d. and maximal values; the number in brackets gives the maximum spatial distance between the prosoma of the spider and the thorax of the fly) at which spiders responded to the fly ($N = 1$–$36$; $n = 2$–$72$). (*b*) Percentages of reactions of spiders to the fly signal at different spatial distances from the fly (vertical distance from platform 5–10 cm) ($N = 12$; $n = 1366$). Filled circles represent percentage response: open bars represent no response: shaded bars represent response.

#### (ii) *Deflection of trichobothria*

Another way to test the significance of air flow produced by a potential prey such as a fly, is to measure the deflection of the trichobothria by the air motion. The distances of the fly from the spider, at which we could still elicit deflection of trichobothria, was considerably larger than those eliciting actual locomotor behaviour towards the prey. As examples, we took three 850 $\mu$m-long trichobothria on different leg segments, kept a spatial distance of 50 cm between the fly and the spider prosoma, and chose an angle $\alpha = 30°$ between the fly (long axis horizontal) and the spider in all cases. Deflection of the trichobothrium set distally on the metatarsal segment of the leg still amounted to roughly 10°, whereas that of the tarsal trichobothrium was roughly 6° and that of the trichobothrium set proximally on the tibia was roughly 3°. Extrapolating these data (see figure 3*a*) to smaller deflection values still considered to effectively elicit a spike response (Reißland & Görner 1985; Zapfel 1992) suggests that distances close to 70 cm are within the trichobothrial air motion detection range. Recent electrophysiological experiments confirm this (A. Höller & F. G. Barth, unpublished data).

As will be seen later (see §3), at an angle $\alpha$ of 30° between the long axis of the fly and the spider, the




PHILOSOPHICAL TRANSACTIONS OF THE ROYAL SOCIETY B BIOLOGICAL SCIENCES

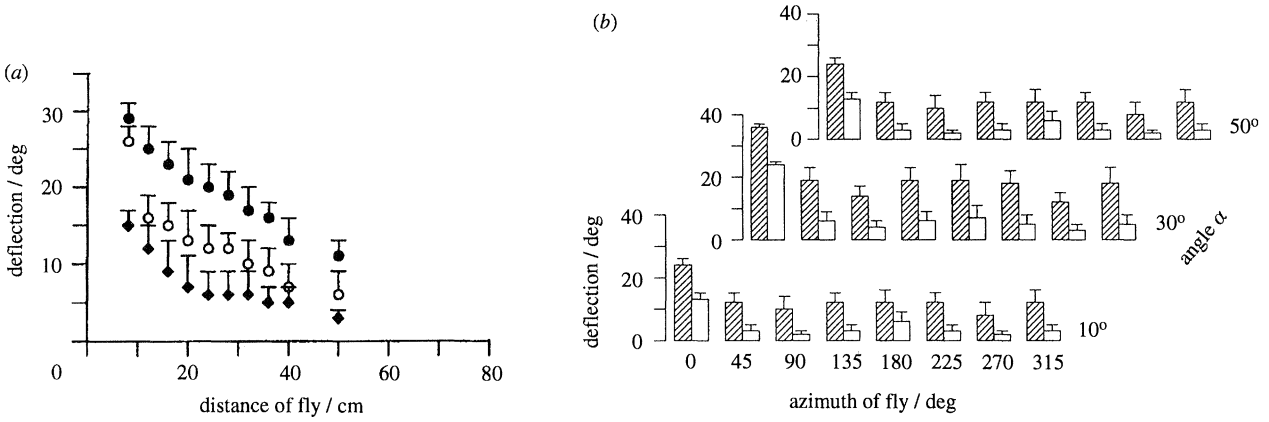


Figure 3. Deflection (average and s.d.) of spider trichobothria by air movement due to a tethered flying fly. (*a*) Deflection of three 850 $\mu$m long trichobothria on different leg segments (tarsus (open circles), metatarsus (filled circles), proximal tibia (filled diamonds)) by air movement produced by fly at different spatial distances and at a constant angle $\alpha$ of 30° formed by the fly and the horizontal spider plane. In this case the spider did not sit on a platform but was mounted on a wired spider-shaped frame allowing the air to pass between the legs ($n = 5$–6). (*b*) Effect on the deflection of tarsal trichobothria: (i) of azimuth of fly position; (ii) of the fly's elevation above the spider given as angle $\alpha$; and (iii) of the presence or absence of a platform under the spider (filled bars = platform; open bars = no platform; $n = 5$–6). An azimuth of 0° refers to a case where the long axis of the fly is aligned with the long axis of the spider leg under study. The spatial distance of fly from spider prosoma was kept constant at 8 cm.

spider is exposed to the highest air movement velocities contained in the fly signal. The longest trichobothrium examined in this experiment measured 1225 $\mu$m, the shortest one only 320 $\mu$m. There is remarkably little difference in average deflection angles among these hairs.

A considerable change in hair deflection angle can be attributed to the presence of a solid substrate, such as a plastic disc 26 cm in diameter on which the spider rests, as opposed to a situation with spaces between the legs permeable to the air flow. Whereas the former situation would be typical of a wandering spider like *Cupiennius* on its dwelling plant, the latter compares to that of a web spider sitting in its web. The platform under the spider increased the deflection angles of the trichobothria considerably (see figure 3*b*). As is seen in §3 the fly signal is also modified under those conditions. When changing the azimuthal angle of the fly it can be seen that an orientation of the fly's long axis in line with the spider leg under study, is the most effective in deflecting the trichobothria (see figure 3*b*).

### (*b*) *Undisturbed air flow around the spider in the wind tunnel*

Profiles of the mean and r.m.s. streamwise velocity component are presented for two air mass flow rates corresponding to bulk average velocities of $V_0 = 0.12$ m s$^{-1}$ (see figure 4*a*) and $V_0 = 0.30$ m s$^{-1}$ (see figure 4*b*), respectively. The profiles were measured along the vertical ($y$) direction at four ($x$, $z$) locations and along the horizontal ($z$) direction at two ($x$, $y$) locations. Defining the Reynolds number as $Re = dV_0/\nu$, where $d$ is a characteristic diameter, and $\nu = 15.69 \times 10^{-6}$m$^2$s$^{-1}$ is the viscosity of air at 27.3 °C, these flow rates correspond to values of the Reynolds number equal to 765 and 1912 when based on the hydraulic diameter of the duct (10 cm), and 84.2 and 210 when based on the diameter of the spider opisthosoma (1.1 cm). We note that the second of the latter two values (210) exceeds the critical value of $Re_c = 130$ for the onset of unsteady motion in the wake of a sphere in free flow. Here, however, the effect of the flat plate supporting the spider will be to dampen significantly the oscillatory component of motion in its wake thus raising the value of $Re_c$. Although the value of $Re_c$ for a system as complex as a spider on a flat plate is not known, present visualization results revealed flow unsteadiness less than 2 Hz in the wake of the spider at the higher of the two speeds ($V_0 = 0.30$ m s$^{-1}$). This flow oscillation frequency (0.5 Hz as suggested by table 1) corresponds to a Strouhal number, $St = fd/V_0$, equal to 0.02, where $f$ is the flow oscillation frequency in Hz, and $d$ the diameter of the opisthosoma.

Although quantitatively different, the qualitative variations of the mean and r.m.s. velocity profiles in figures 4*a* and *b* are quite similar for the same coordinate locations. The two mean velocity profiles measured along (30, $y$, 0) are 30 mm downstream of the plate leading edge and 17 mm upstream of the spider's prosoma. As expected, near the plate the variation with $y$ of the high flow rate profile is steeper than that for the low flow rate. The shapes of these two profiles suggest approximate boundary layer thicknesses $\delta$ at $x = 30$ mm corresponding to $\delta = 12$ mm for the low flow rate and $\delta = 8$ mm for the high.

In contrast, the corresponding profiles measured along (94, $y$, 0), 17 mm downstream of the opisthosoma, show the strong effect produced by the spider's body as an obstruction in the path of the flow. At both flow rates, the streamwise component of velocity is drastically reduced for values of $y$ less than 14 mm. The absence of negative velocities in this profile for values of $y$ larger than 5 mm suggests that either the recirculating flow region that exists in the wake of the spider's body is less than 5 mm high at $x = 94$, or that the $x$ coordinate location of this profile lies beyond the recirculating flow region. An inspection




PHILOSOPHICAL TRANSACTIONS OF THE ROYAL SOCIETY B BIOLOGICAL SCIENCES

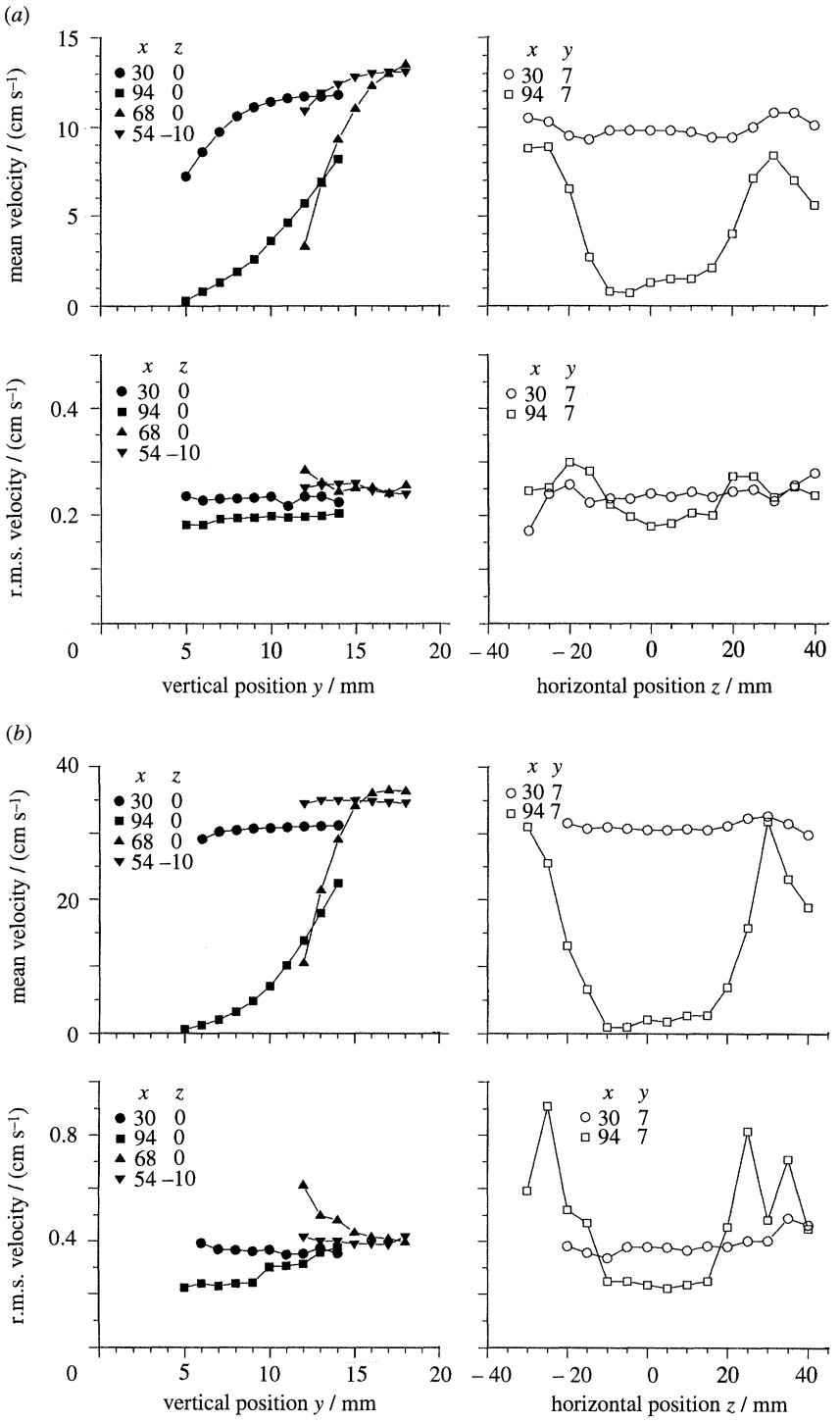


Figure 4. Laser-Doppler measurements of mean and r.m.s. streamwise velocity component profiles corresponding to the undisturbed air flow (*a*) $V_0 = 12$ cm s$^{-1}$; and (*b*) $V_0 = 30$ cm s$^{-1}$, around the spider. The leading edge of the spider platform corresponds to $x = 0$; the spider prosoma begins at $x = 47$ mm; the opisthosoma ends at $x = 77$ mm; the spider is 10 mm in width at the widest point on the opisthosoma and 10 mm in height at the highest point on the prosoma. A horizontal position of $z = 0$ indicates a position of the measuring probe above the long axis of the spider. Position of measuring profiles relative to spider as follows. Vertical profiles: filled circles, 17 mm in front of spider prosoma; filled squares, 17 mm behind opisthosoma; filled upright triangles, above opisthosoma; filled inverted triangles, at level of prosoma but 10 mm away from body long axis above leg; horizontal profiles: open circles, 17 mm in front of prosoma, and 7 mm above platform; open squares, 17 mm behind opisthosoma and 7 mm above platform.

of the visualization results for a case with $V_0 = 0.12$ m s$^{-1}$ confirms that the former is the case.

The mean velocity profiles measured along the horizontal or spanwise ($z$) coordinate direction further confirm the above findings. The profiles measured along (30, 7, $z$) show that the flow approaching the spider is fairly uniform along the $z$ coordinate direction, while the profiles measured along (94, 7, $z$) reveal strong reductions in the streamwise component of velocity in the wake of the spider. However, closer inspection uncovers an interesting detail in these profiles. The horizontal profiles measured both up-

Table 1. *Air flow around the spider in the wind tunnel*

(Reynolds (*Re*) and Strouhal (*St*) numbers for wind tunnel, spider opisthosoma and spider leg. $Re_{crit}$ = critical values of Reynolds number according to van Dyke (1982); $St_m$ = Strouhal number determined from present visualization observations; $St_c$ = Strouhal number calculated for a sphere (approximating the opisthosoma $d = 1.1$ cm) (Clift *et al.* 1978) or a cylinder (approximating leg $d = 0.2$ cm) (White 1991) in free flow. Values in brackets are oscillation frequencies.)

| | $V_0 = 12$ cm s$^{-1}$ | | | | $V_0 = 30$ cm s$^{-1}$ | | | |
|---|---|---|---|---|---|---|---|---|
| | $Re_{crit}$ | $Re$ | $St_m$ | $St_c$ | $Re_{crit}$ | $Re$ | $St_m$ | $St_c$ |
| wind tunnel | | 765 | | | | 1912 | | |
| spider opisthosoma | 130 | 84.2 | 0 (0 Hz) | 0 (0 Hz) | 130 | 210 | < 0.02 (< 0.5 Hz) | 0.04 (1.1 Hz) |
| spider leg | 40 | 15.3 | 0 (0 Hz) | 0 (0 Hz) | 40 | 38.2 | < 0.01 (< 1.5 Hz) | < 0.03 (< 4.5 Hz) |

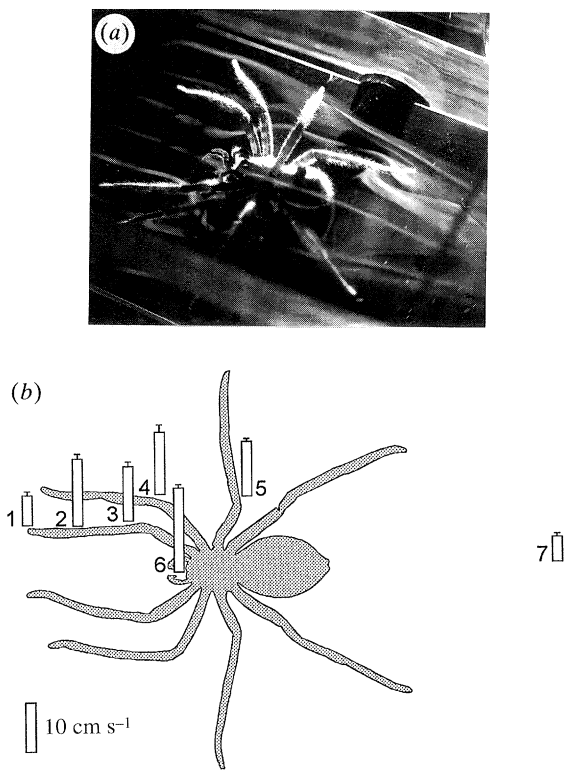


Figure 5. Undisturbed air flow around a spider; flow rate $V_0 = 12$ cm s$^{-1}$, spider oriented horizontally and with long axis parallel to air flow. (*a*) Flow visualization reveals an asymmetric recirculating flow region in the wake of the opisthosoma and strong curvature of the smoke streaklines in and around the spaces defined by the spider legs. (*b*) Air speeds measured immediately above different areas of the spider body and behind it. Geometrical arrangement of spider as in (*a*).

stream and downstream of the spider show flow accelerations for absolute values of $z$ larger than 25 mm, approximately. In addition, the profiles measured downstream of the spider show flow decelerations for absolute values of $z$ greater than 30 mm. These effects are attributed to the influence of the spider's front and back legs on the approaching and departing flows, respectively.

That the legs strongly affect the flow is supported by the corresponding (horizontal) r.m.s. velocity profiles. In particular, the profiles measured along (94, 7, $z$) indicate increases in the flow r.m.s. intensity (the r.m.s. velocity divided by the local mean velocity) ranging from 65% for the low flow rate (0.12 m s$^{-1}$) to 270% for the high (0.30 m s$^{-1}$). Given the steady streamlined (laminar) nature of the approaching flow, these remarkable increases in the r.m.s. are attributed to the unsteadiness associated with oscillations of the recirculating flow around the legs, a finding confirmed by the flow visualization results (see figure 5*a*). The flow unsteadiness is not unexpected as a characteristic value of the Reynolds number, $Re = dV_0/\nu$, based on the diameter of a spider leg (2 mm, approximately) yields a value of 38.2 when $V_0 = 0.30$ m s$^{-1}$. This value falls in the critical range 35–40 required for the onset of mild flow unsteadiness, in the wake of a cylinder in cross-flow. In this case, the situation is rendered quite complex due to local accelerations and decelerations of the air flowing over the spider's body, and around the irregular spaces among the various legs. Inspection of the smoke streaklines in figure 5*a* shows that the complicated geometry of the spider's body induces strong streamline curvature and regions of flow reversal downstream of both the opisthosoma and several locations on the legs.

Vertical profiles of the mean velocity were also measured along (68, $y$, 0), above the opisthosoma, and along (54, $y$, −10), to the side of the spider's body. For both bulk velocity conditions, the profiles show similar trends, namely: (i) a strong deceleration of the flow in the boundary layer that develops over the spider's body; and (ii) accelerations of the flows passing between the spider's body and the tunnel side wall, and above the boundary layer that develops over the body. As expected, all these effects are more pronounced for the high speed flow than for the low speed flow.

The r.m.s. profiles measured along the vertical coordinate direction are also quite similar for the two bulk flow rates. The profiles determined along (30, $y$, 0) confirm that the approaching flows at both $V_0 =$ 0.12 m s$^{-1}$ and 0. 30 m s$^{-1}$ are streamlined and laminar, having r.m.s. intensities less than ca. 3.5% and 1.5% for the low and high speed flows, respectively. In contrast, the vertical profiles along (94, $y$, 0), downstream of the spider, reveal that at low values of $y$ (less than 10 mm), near the plate, the flow in the spider's wake has much larger values of the r.m.s. intensity at $V_0 = 0.30$ m s$^{-1}$, than at $V_0 = 0.12$ m s$^{-1}$. This is attributed to the flow unsteadiness expected in the spider's




PHILOSOPHICAL TRANSACTIONS OF THE ROYAL SOCIETY B BIOLOGICAL SCIENCES

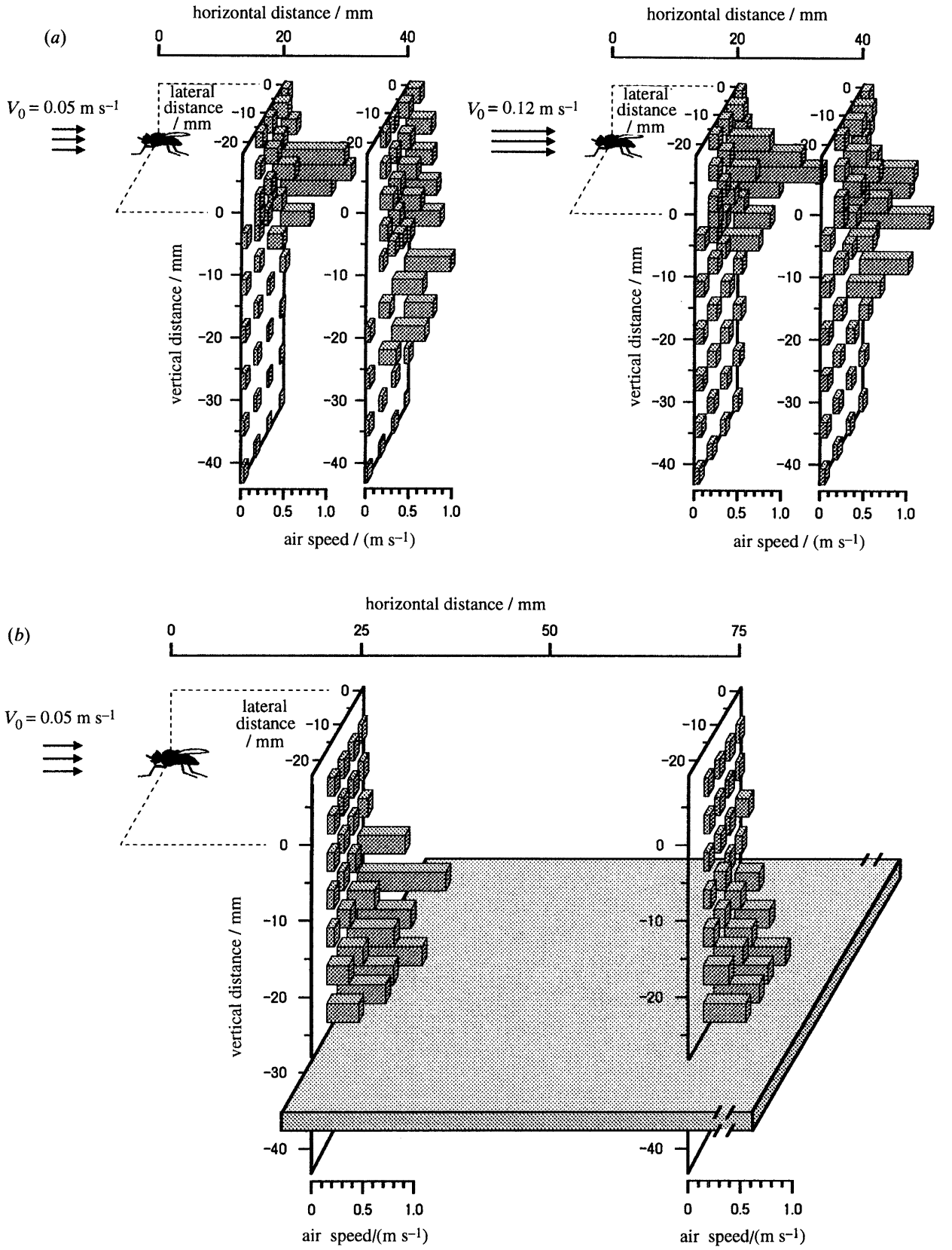


Figure 6. Air flow produced by active tethered fly measured with a laser-Doppler-velocimeter in the wind tunnel. (*a*) Air velocity profiles 20 mm and 40 mm behind the fly with laminar background flow of 0.05 m s$^{-1}$ (left) and 0.12 m s$^{-1}$ (right), respectively. (*b*) Air flow produced by active fly measured above a plate 25 mm and 75 mm behind the fly with laminar background flow of 0.05 m s$^{-1}$.

wake at the higher of the two Reynolds numbers investigated, and is confirmed by the flow visualization results. The r.m.s. profiles measured above and to the side of the spider correspond to regions of flow with relatively large velocity so that at these locations the relative r.m.s. is low.

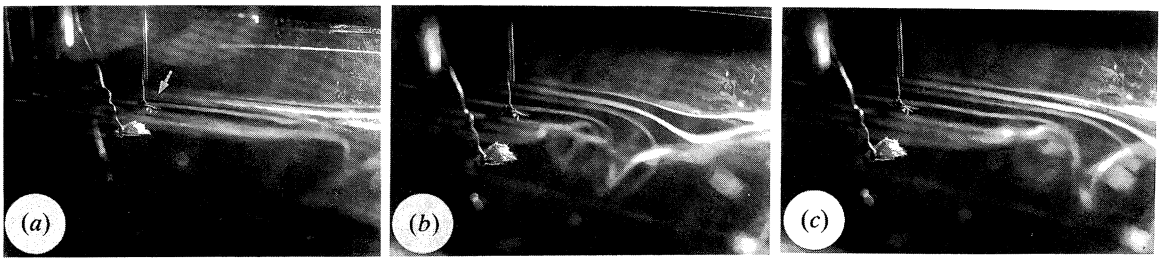


Figure 7. Visualization of air flow streaklines produced by stationarily flying fly (arrow). Experiment was performed in the wind tunnel shown in figure 1 with $V_0 = 0.12$ m s$^{-1}$. In the photograph sequence the flow is from left to right and the time interval between photographs is 0.25 s. The streak lines originate at the level of the fly and illustrate the highly vortical and unsteady nature of the fly-generated flow which completely alters the weaker background flow.

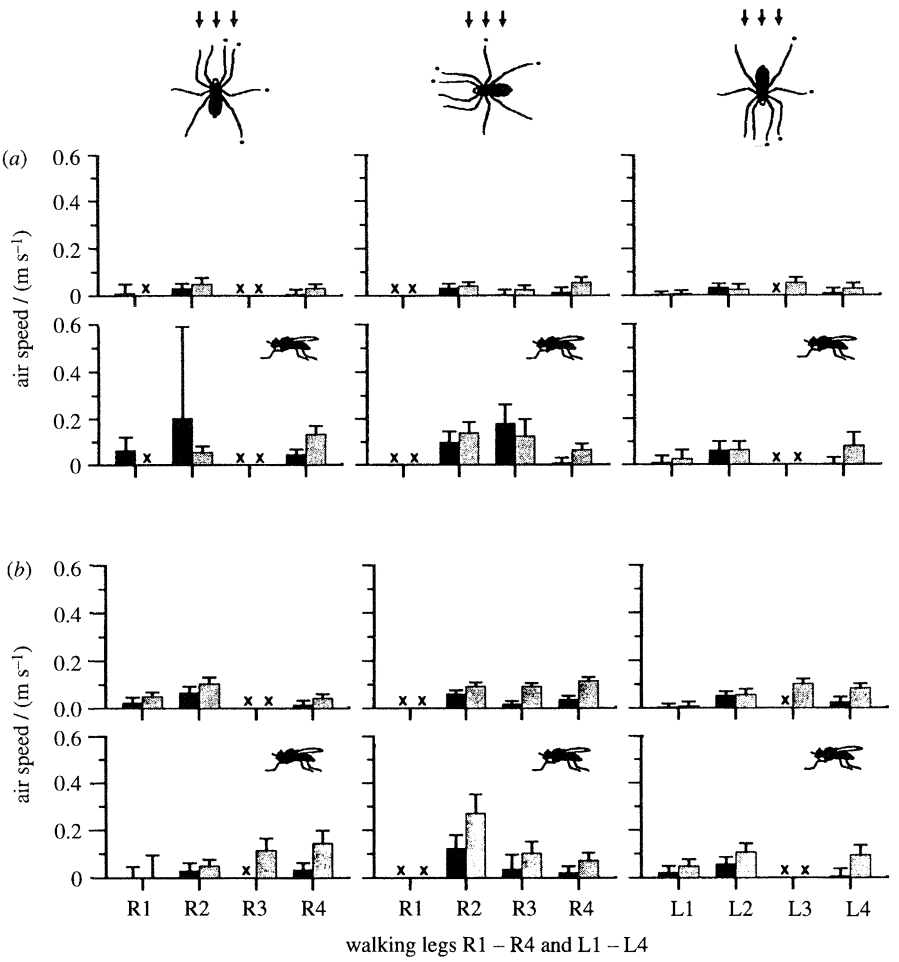


Figure 8. Flow around spider without and with the active fly. Mean and r.m.s. velocities were measured above the tarsus (dark bars) and metatarsus (bright bars) of a spider sitting on a platform in the wind tunnel with background flow rates of (*a*) 0.05 m s$^{-1}$ and (*b*)0.12 m s$^{-1}$. Arrows indicate direction of background air flow, whereas the dots mark the legs examined. $R_{1-4}$ right legs, $L_{1-4}$ left legs; crosses (x) indicate cases where measurement was not possible for geometrical obstruction reasons. Position of fly was 25 mm in front of platform edge and 30 mm above platform.

Additional measurements of the mean and r.m.s. velocities were made at selected ($x$, $y$, $z$) coordinate locations near to and around the spider (see figure 5*b*).

### (*c*) *Air flow due to the fly*

#### (i) *The fly signal*

LDV measurements of the streamwise velocity component, obtained with an active fly tethered in the wind tunnel, are shown in figure 6. The measurements were made both without (see figure 6*a*) and with (figure 6*b*) the platform in place. In all cases the fly was tethered in the vertical symmetry plane of the duct and at a distance 3 cm from the top wall. With the plate present, the fly was placed at an $x$ location 25 mm ahead of the plate's leading edge and was located 28 mm above it.

Velocity profiles measured along the spanwise ($z$) coordinate direction revealed a flow which was fairly symmetrical with respect to the duct vertical symmetry

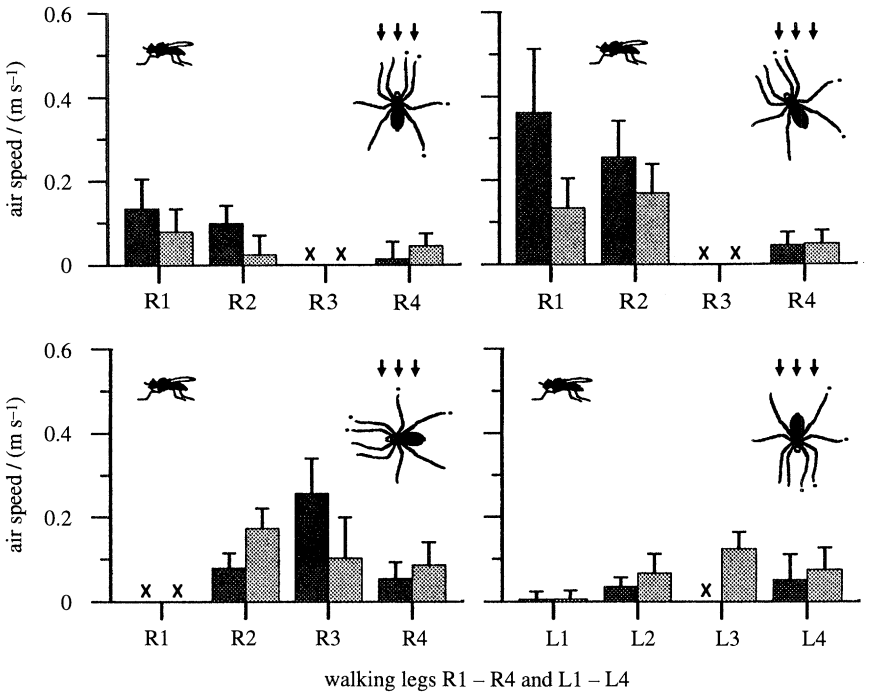


Figure 9. Flow around spider with active fly and with different spider orientation. Arrows give direction of background flow (0.12 m $s^{-1}$). Dark bars refer to measurement above tarsi, bright bars to those above metatarsi of legs indicated by dots in insets. Position of fly: 25 mm in front of spider platform edge and 25 mm above it. Crosses (x) indicate cases where measurement was not possible for geometrical obstruction reasons.

plane ($z = 0$). For this reason the bulk of the mean (and r.m.s.) velocity measurements were restricted to the half symmetry plane shown in the figures. In the configuration without the plate two cases with background flows corresponding to $V_0 = 0.05$ and 0.12 m $s^{-1}$ were investigated. For the configuration with the plate only the flow with $V_0 = 0.05$ m $s^{-1}$ was explored.

In all cases the results obtained reveal a field of relatively concentrated unsteady high speed flow, of the order of 1 m $s^{-1}$, immediately behind the fly. The flow is directed downwards from the fly, and is contained in a cone-like region of influence bounded by its angle with respect to the horizontal passing through the fly and contained in the vertical symmetry plane ($\alpha$), and a spanwise ($z$-direction) spread angle centered on the vertical symmetry plane ($\beta$). In the absence of the plate (see figure 8*a*) we find: $\alpha = 33° \pm 2°$ and $\beta = 40° \pm 2°$ when $V_0 = 0.05$ m $s^{-1}$; $\alpha = 27° \pm 2°$ and $\beta = 26° \pm 2°$ when $V_0 = 0.12$ m $s^{-1}$. It is clear from these values of $\alpha$ and $\beta$, and from the magnitudes of the air speeds measured at the furthest (40 mm) downstream location, that the solid angle of the fly's cone of influence is smaller, and the speed of the flow contained in it stronger, in the case of the higher background flow. From this we readily conclude that a steady background flow works to confine and project further, the flow field generated by the fly, and that a high background flow does so more effectively than a low one. With the plate present, the corresponding angles are $\alpha = 45° \pm 2°$ and $\beta = 53° \pm 2°$ when $V_0 = 0.05$ m $s^{-1}$. These values are significantly larger than $\alpha = 33°$ and $\beta = 40°$ ($V_0 = 0.05$ m $s^{-1}$, no plate) demonstrating the major effect of the plate, especially on the spanwise or lateral spread of the fly-induced flow field.

The above angle findings are in good qualitative agreement with the visualization results obtained for similar flow conditions (see figure 7) and with our experiments on the sensory space described in §1. Photographic and video recordings of the flow, show it is highly vortical and oscillatory in the wake of the fly. Measurements of the r.m.s. velocity, corresponding to the conditions and locations of figure 6 (not plotted here), also revealed a cone of influence of similar dimensions to that of the mean velocity. Velocity fluctuations as large as 56% of the local mean velocity were detected in the flow reaching the leading edge of the plate. In traversing the length of the plate, from the 25 mm to the 75 mm location in figure 6, the fluctuation levels decayed to values less than 32%. In absolute terms, those percentages translate to 0.25 m $s^{-1}$ (r.m.s.) and 0.125 m $s^{-1}$ (r.m.s.), respectively, and represent fairly large fluctuations of the local mean velocity.

That the flow in the wake of the fly should be highly unsteady and vortical (see figures 6*a*, *b* and 7) is to be expected from what is known of the aerodynamics of insect flight. In the process of generating lift by wing flapping, not only is the flow pulsed periodically but vortices are shed from the tip of the wing (Maxworthy 1981). Large values of the r.m.s. velocity result from the fluctuations superimposed on the mean flow which itself is directed at an angle and downwards.

(ii) *Flow around the spider with the fly*

Measurements of the mean and r.m.s. (see bars) velocity near the spider's legs are shown in figure 8*a* and *b* for background flows corresponding to $V_0 = 0.05$ and $V_0 = 0.12$ m $s^{-1}$, respectively, and for different relative orientations of the spider with respect to the

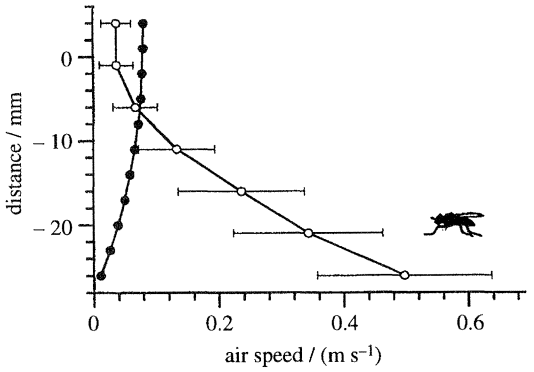


Figure 10. Vertical profiles of streamwise velocity above centre of platform in the test section of the wind tunnel shown in figure 1. Filled circles = laminar air flow ($V_0$ = 0.08 m s$^{-1}$); open circles: stationarily flying fly (bars give r.m.s. values). The position of the horizontally oriented platform corresponded to $y = -28$ on the ordinate, that of the fly to $y = 0$ and 75 mm ahead of the point of measurement of the velocity profiles.

approaching flow. For each leg, two values of velocity are shown in the plots: for a location immediately above the tarsus and above the metatarsus.

The data in figure 8*a* with $V_0 = 0.05$ m s$^{-1}$ show that, for all three orientations of the spider with respect to the approaching flow, practically all the locations successfully probed over the legs are exposed to the high speed flow induced by the fly. In contrast, with $V_0 = 0.12$ m s$^{-1}$ (see figure 8*b*), only a few of the measurement locations are exposed to velocities higher than the background flow. Additionally, it is revealed that the R1 and R2 locations correspond to the L1 and L2 locations, the difference being the orientation of the spider with respect to the approaching flow (see figure 9). In the case of L1, L2, these locations lie in the slow moving wake of the spider and, being thus protected, are less sensitive to the approaching flow. For the same reason, the velocity sensitivities of R4 and L4 are interchanged.

When facing a fly directly, or in a position set at right angles to it, the speed of the flow reaching the spider's legs is substantially higher in the presence of an active fly. In the forward facing orientation, the first and second legs appear to be most strongly affected by the fly-induced flow, when at right angles, the second and third legs are affected more.

Measurement of vertical streamwise velocity profiles above the platform, without the spider, (see figure 10) clearly demonstrates the enormous impact of the fly

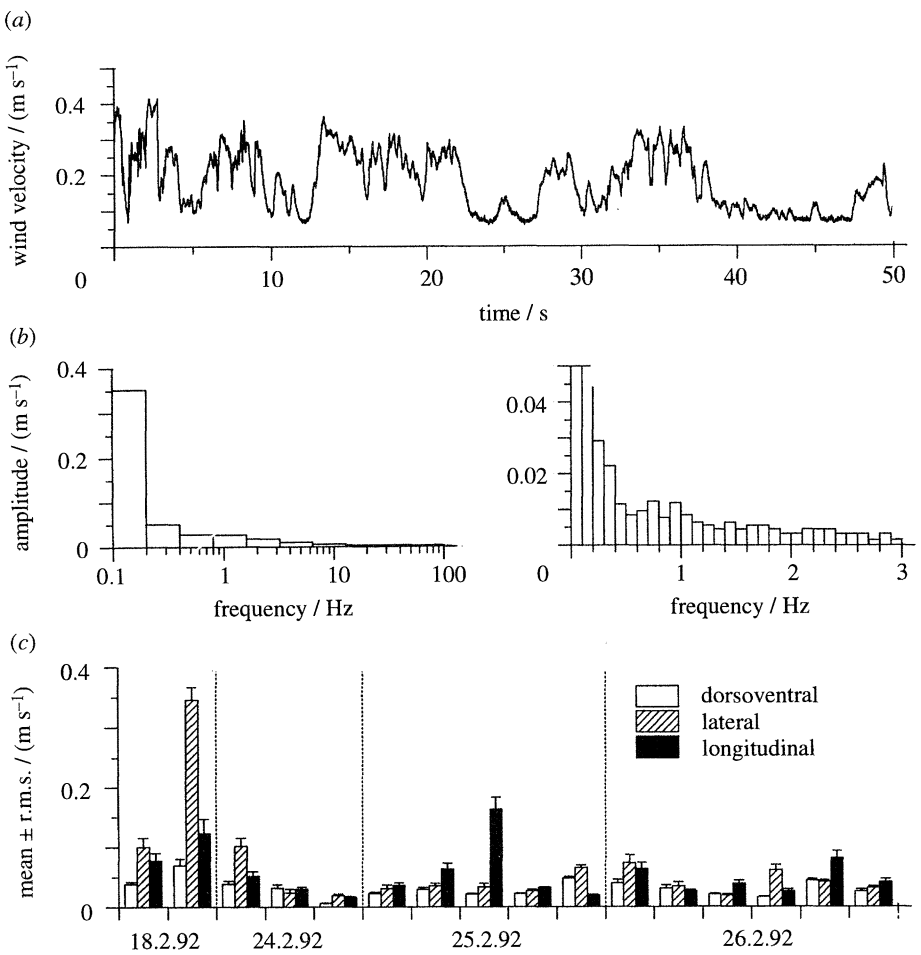


Figure 11. Air movement in the natural habitat. Wind velocities were measured approximately 1 cm above the spider prosoma in the longitudinal, lateral, and dorso-ventral direction relative to the spider. Spiders ($N = 11$) sat on their natural dwelling plants to catch prey. All measurements were taken after sundown with spiders sitting on bromeliads (February 18, 24, and 26) or on the pseudostem of banana plants (February 25). The example given in (*a*) (real time recording for 50 s) and (*b*) (frequency spectra) was chosen to demonstrate the case with the highest average wind velocity of all 16 measured and summarized in (*c*). (February 18, lateral air movement).




PHILOSOPHICAL TRANSACTIONS OF THE ROYAL SOCIETY B BIOLOGICAL SCIENCES

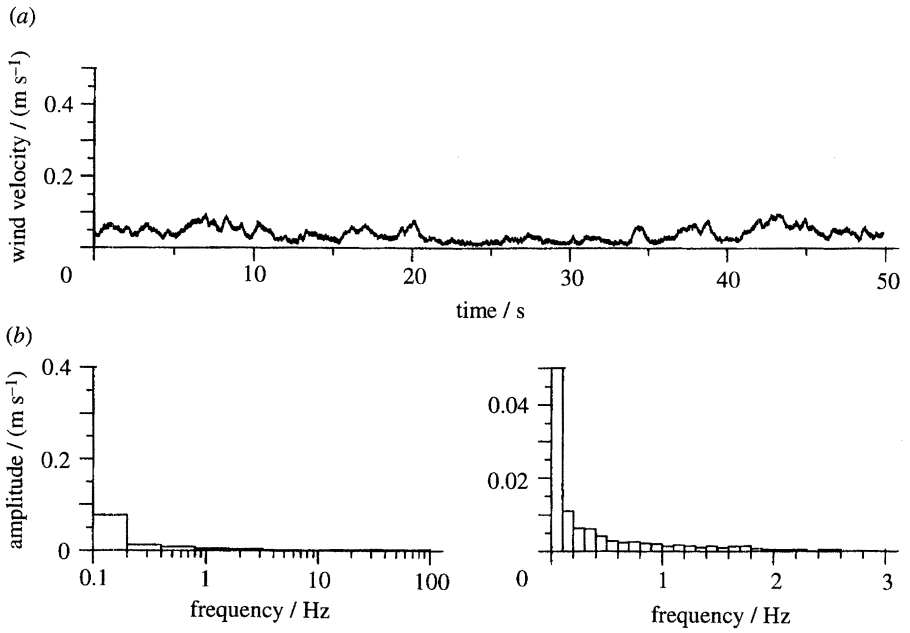


Figure 12. Air movement in the field above spider in its natural habitat on a bromeliad after sundown. (*a*) Analogue velocity reading for a 50 s interval; (*b*) frequency spectra of same recording with different resolution. The example chosen demonstrates a case typical for a low average wind velocity (February 24, longitudinal movement; see figure 11*c*).

signal. Not only is there a considerable increase of the average air particle velocity close to the surface of the platform, but the large r.m.s. values also indicate high unsteadiness in the air movement produced by the flight of a tethered fly.

### (*d*) *Background noise in the field*

The measurements reported in this section were made to get an idea of the characteristic air flow velocities and air flow fluctuations to which *Cupiennius* is exposed in its natural habitat when sitting on its dwelling plant (bromeliads, banana plant) after sundown and when ambushing prey (Barth *et al.* 1988).

The most general observation we made when studying this problem in February 1992 in Costa Rica, was that wind velocities and the occurrence of gusts as a rule dropped significantly shortly after sunset, i.e. at the time when *Cupiennius* leaves its retreat to sit openly on its dwelling plant waiting for prey (Seyfarth 1980).

The actual air-flow measurements taken roughly 1 cm above a spider's prosoma were characterized by both low velocities and the predominance of very low frequencies. Figure 11 illustrates this, showing the representative results of 16 measurements obtained with 11 spiders on four different days. Mean wind velocities are below 0.1 m s$^{-1}$, typically with less than 15% r.m.s. fluctuation. The frequency spectra (see figures 11 and 12) in the great majority of cases are dominated by frequencies below 10 Hz, and occasionally lower than 3 Hz. Only in exceptional cases did the spectra contain frequencies higher than 10 Hz or even higher than 20 Hz.

## DISCUSSION

### (*a*) *Range of the trichobothria*

Görner & Andrews (1969) classified the sense mediated by trichobothria as 'touch at a distance' using a term originally coined by Dijkgraaf (1947) for the lateral line organs of fish and amphibia, another medium displacement sensitive system. The message behind this definition is how importanct it is to distinguish far-field pressure receivers from near-field displacement receivers. To talk about 'touch' may be misleading, however, considering that *Cupiennius salei* shows a behavioural response to a buzzing fly more than 25 cm away and that its trichobothria are deflected by such a signal even at a distance of 70 cm or more. This latter value is identical to the maximal distance from which the nearfield of a flying wasp can stimulate the sensory cell of displacement sensitive hairs on the *Barathra* caterpillar (Tautz & Markl 1978). It has been repeatedly reported that spiders catch free-flying insect prey while these are still in the air. This is also true in the case of *Cupiennius salei*, which probably uses its trichobothria not only for the detection of prey, but for the detection of predatory wasps (Pompilidae) and parasitic neuropterans (Mantispidae) also. We have observed the approach of such enemies in the field repeatedly: the spider reacts to them by raising its front legs, in seemingly defensive behaviour.

This is not to say that flying insects are the only or even predominant source of stimulation for the trichobothria of *Cupiennius salei* and its close relatives (Lachmuth *et al.* 1984). For these wandering spiders, insects crawling over their dwelling plant will be the more common prey. Notwithstanding the importance of the substrate borne vibrations (Barth 1985), the trichobothria will be stimulated by the air movement accompanying the locomotory movements of prey




PHILOSOPHICAL TRANSACTIONS OF THE ROYAL SOCIETY B BIOLOGICAL SCIENCES

from distances of 1–3 cm (Den Otter 1974; Camhi *et al.* 1978; Reißland & Görner 1978; Gnatzy & Kämper 1990).

### (*b*) *Undisturbed air flow around the spider*

One of the main problems to be solved by any sensory system is that of filtering the biologically relevant signals from background noise. Differences in amplitude, frequency content, and/or temporal pattern are often found to differ in these two cases. Considering the likelikood of a two- or even three-dimensional analysis of complex air-movement patterns by approximately 1000 trichobothria distributed over a large area of the spider, the question arises: what does the air flow undisturbed by a prey or predator signal look like? From the fluid mechanical point of view, a spider is a complex geometrical structure. The flow pattern visualized and measured in laminar flow at velocities close to those of the background flow found in the field (see below) can be used to indicate a few important qualitative effects.

One of these effects is the uneven distribution of the time-averaged velocity over different areas of the spider body (see figures 4 and 5). With the air flow approaching from the front, both the mean and r.m.s. values of velocity are slightly higher above the legs than above the spider pro- and opisthosoma. This is to be expected: because of their large length to diameter ratio, the legs protrude into higher velocity regions of flow less affected by the spider's body. In a sense, the legs facing the approaching flow sample different vertical segments of the velocity profile as a function of leg height. In the wake behind the spider opisthosoma, however, the mean velocity (less so the r.m.s.) is markedly decreased to values close to zero. Thus, even under the simple conditions of laminar flow considerable velocity gradients develop around the spider. The pattern of these gradients is even more complicated when considering a change in the spider's horizontal orientation with respect to the main flow direction (see figure 8). It is important, then, to note that for flow approaching the spider directly from the front or the back, the flow around the spider is symmetrical (with respect to a symmetry plane dividing the spider in half). For flow approaching the spider laterally, the flow symmetry is lost, the motion of air on the leeward side of the spider being considerably more vortical and unsteady than on the windward side, as a result of the cumulative effects of the spider's body and legs.

The details of velocity distribution may be too variable to be used by the spider for the identification and location of stimulus sources. From the general patterns, i.e. the symmetry or asymmetry in the excitation of the trichobothria on the eight legs and pedipalps, its sequential occurrence and differences in unsteadiness (s.a) the spider may nevertheless infer where the wind comes from. The regular and stereotyped arrangement of its extremities would assist such an ability which has not yet been experimentally demonstrated in spiders, but is known for scorpions (Linsenmair 1968). Although the spider is more or less equally sensitive in all horizontal directions (see figure 2) facing the background wind may be advantageous for prey capture because the prey signals will be carried, preferentially, towards the anterior side of the spider by the background flow, and the spider needs to make only the slightest turn towards the prey.

According to our field measurements of the air flow above the spider sitting in its prey capture posture, on its natural dwelling plant, during its nightly period of activity, velocities below 0.1 m $s^{-1}$ are most typical. Larger velocities, up to almost 0.4 m $s^{-1}$, occurred only twice among the 16 cases measured. The velocities chosen for the wind tunnel experiments therefore were in the biologically relevant range.

### (*c*) *Prey signals*

The difference between the background flow and the fly signal is remarkable. Apart from the concentrated nature of the fly signal, this applies to both the mean and r.m.s. velocities. With the fly present, air speeds close to 1 m $s^{-1}$ are reached in the near wake, 40–75 mm downstream of the fly. Corresponding values of the r.m.s. are as large as 0.25 m $s^{-1}$, yielding fluctuation intensities of the order of 25 % compared to 2–3 % for the completely unperturbed background flow. Although the prosoma, opisthosoma and, especially, legs of the spider are also capable of significantly altering the background flow (see figure 8), the frequencies of these oscillations are, typically, at most a few Hertz, compared to flow oscillation frequencies of the order of 100 Hz produced by the fly. Also, in absolute terms, the fly-induced flow oscillations are at least equally energetic when compared with those induced by the spider's body. From this we conclude that the interference of the spider's body with the background flow will not significantly distort the fly signals reaching it. Also, r.m.s. values of the background wind measured in the field are lower than those of the fly signal (typically $< 15\,\%$).

A cockroach or cricket passing or approaching *Cupiennius* is detected by the substrate-borne vibrations it produces in the plant from large distances (Barth 1985). When the prey animal is very close (1–2 cm) to a spider leg, the air movement produced and detected by trichobothria will add to the effect of the plant vibrations (Den Otter 1974; Reißland & Görner 1978; Hergenröder & Barth 1983*b*.). The signal received by the spider in such a case differs from the fly signal described above by its localized character as well as by its comparatively low (below 20 Hz) frequency contents and low air particle velocities (up to approximately 2 cm $s^{-1}$) (Camhi *et al.* 1978; Gnatzy & Kämper 1990). The spider probably identifies them as prey-like, different from background by its pulsed nature. We assume that, not unlike the findings for the reception of substrate borne vibrations, an effective airborne prey stimulus is characterized by: a relatively broad bandwidth, frequencies higher than those contained in the background air flow, and an irregular time course. Regarding the spider's task of identifying the direction of a source of air movement it should be noted that the stimulation patterns, to which the ensemble of trichobothria on the different legs and




PHILOSOPHICAL TRANSACTIONS OF THE ROYAL SOCIETY B BIOLOGICAL SCIENCES

pedipalps are exposed, have directional properties under all three circumstances considered: the undisturbed air flow around the spider, the air movement generated by the fly, and the air movement due to the movements of an insect walking on the spider's dwelling plant. Steady background flow may increase this directionality by confining the perturbed flow fields.

Although present flow visualization and point measurements of velocity suggest highly unsteady, vortical states of motion in the wake of a fly, the time-averaged data do not allow an unambiguous identification of the particular amplitude and/or frequency content eliciting prey capture behaviour in the spider. For the same reason the air velocity signals cannot be associated with their mechanistic origins in the fly. Flies, like other insects, beat their wings to generate lift and thus overcome their mass. The result is a downwards directed mean flow which is at an angle with respect to the horizontal and therefore provides for forward movement. The down and up wingstrokes both involve large amplitudes of angular movement of the wings with big twists at each extreme of the oscillation. Each stroke sheds tip vorticity in the form of an incomplete vortex ring and the sequence of these rings bounds a jet-like flow with strong mean velocity and large levels of unsteadiness (Ellington 1984). The spider extracts the information necessary to identify its prey from this highly complex flow pattern. Continuing work has to show which aspects of the air velocity signal are indeed used by the spider.

Our research was generously supported by the Austrian Science Foundation (FWF P 7882-B and P 9336-B to F.G.B.). Additional support from the Committee on Research at the University of California at Berkeley is gratefully acknowledged. Thanks to D. Baurecht and A. Schmitt for their contribution to the measurements in the field and to B. Treidler and S. Wragg for their help with the LDA measurements in the wind tunnel. Dipl.Ing. R. Machan and Ing. A. Szpetkowski developed a very handy anemometer for our field work. A grant of the Austrian Ministry for Science and Research enabled U.W. to spend several months in J.A.C.H's laboratory, Berkeley. We also thank an anonymous referee for helpful comments on the wake of the fly and the OTS for its support at its field station in Las Cruces, Costa Rica.

## REFERENCES

Barth, F.G. 1985 Neuroethology of the spider vibration sense. In *Neurobiology of Arachnids* (ed. F.G. Barth), pp. 203–229. Berlin: Springer-Verlag.

Barth, F.G. & Geethabali, 1982 Spider vibration receptors. Threshold curves of individual slits in the metatarsal lyriform organ. *J. comp. Physiol.* **148**, 175–185.

Barth, F.G., Nakagawa T. & Eguchi, E. 1993 Vision in the ctenid spider *Cupiennius salei*: spectral range and absolute sensitivity. *J. exp. Biol.* **181**, 63–79.

Barth, F.G., Seyfarth, E.-A., Bleckmann, H. & Schüch, W. 1988 Spiders of the genus *Cupiennius* SIMON 1891 (Araneae, Ctenidae). I. Range distribution, dwelling plants, and climatic characteristics of the habitats. *Oecologia* **77**, 187–193.

Barth, F.G., Wastl, U, Humphrey, J.A.C & Devarakonda, R. 1993 Dynamics of arthropod filiform hairs. II. Mechanical properties of spider trichobothria (*Cupiennius salei* KEYS.). *Phil. Trans. R. Soc. Lond.* B **340**, 445–461.

Boyan, G.S. & Ball, E.E. 1990 Neuronal organization and information processing in the wind-sensitive cercal receptor/giant interneurone system of the locust and other orthopteran insects. *Prog. Neurobiol.* **35**, 217–243.

Camhi, J.M. 1980 The escape system of the cockroach. *Scient. Am.* **243**, 144–156.

Camhi, J.M. & Tom, W. 1978 The escape behaviour of the cockroach *Periplaneta americana*. I. Turning response to wind puffs. *J. comp. Physiol.* **128**, 193–201.

Camhi, J.M., Tom, W. & Volman, S. 1978 The escape behaviour of the cockroach *Periplaneta americana* L. II Detection of natural predators by air displacement. *J. comp. Physiol.* **128**, 203–212.

Clift, R., Grace, J.R. & Weber, M.E. 1978 *Bubbles, Drops and Particles*. New York: Academic Press.

Dambach, M. & Heinzel, H.-G. 1985 Niederfrequente Luftschwingungen als mögliche Kommunikationssignale bei einer Grille. *Verh. dt. Zool. Ges.* **78**, 333.

Dambach, M., Rauscha, H.-G. & Wendler, G. 1983 Proprioceptive feedback influences the calling song of the cricket. *Naturwissenschaften* **70**, 417.

Den Otter, C.J. 1974 Setiform sensilla and prey detection in the bird-spider *Sericopelma rubronitens* Ausserer (Araneae, Theraphosidae). *Neth. J. Zool.* **24**, 219–235.

Dijkgraaf, S. 1947 Über die Reizung des Ferntastsinnes bei Fischen und Amphibien. *Experientia* **3**, 206–208.

Dyke van, M. 1982 *An album of fluid motion*. Stanford, California: The Parabolic Press.

Ellington, C.P. 1984 The aerodynamics of hovering insect flight. Parts 1 to 6. *Phil. Trans. R. Soc. Lond.* B **305**, 1–181.

Gnatzy, W. & Kämper, G. 1990 Digger wasp against crickets. II. An airborne signal produced by a running predator. *J. comp. Physiol.* **167**, 551–556.

Görner, P. & Andrews, P. 1969 Trichobothrien, ein Ferntastsinnesorgan bei Webespinnen (Araneen). *Z. vergl. Physiol.* **64**, 301–317.

Hergenröder, R. & Barth, F.G. 1983*a* Vibratory signals and spider behavior: How do the sensory inputs from the eight legs interact in orientation? *J. comp. Physiol.* **152**, 361.-371.

Hergenröder, R. & Barth, F.G. 1983*b* The release of attack and escape behavior by vibratory stimuli in a wandering spider (*Cupiennius salei* Keys.). *J. comp. Physiol.* **152**, 347–358.

Hoffmann, Ch. 1967 Bau und Funktion der Trichobothrien von *Euscorpius carpathicus* L. *Z. vergl. Physiol.* **54**, 290–352.

Humphrey, J.A.C, Devarakonda, R., Iglesias, I. & Barth, F.G. 1993 Dynamics of arthropod filiform hairs. I. Mathematical modelling of the hair and air motions. *Phil. Trans. R. Soc. Lond.* B **340**, 423–444.

Lachmuth, U., Grasshoff, M. & Barth, F.G. 1984 Taxonomische Revision der Gattung *Cupiennius* SIMON 1891 (Arachnida; Araneae). *Senckenberg. biol.* **65**, 329–372.

Linsenmair, K.E. 1968 Anemotaktische Orientierung bei Skorpionen (Chelicerata, Scorpiones). *Z. vergl. Physiol.* **60**, 445–449.

Maxworthy, T. 1981 The fluid dynamics of insect flight. *A. Rev. Fluid Mech.* **13,** 329–350.

Nachtigall, W. 1973 Investigation of wing movements and the generation of aerodynamic forces in flying Diptera. In *Comparative physiology* (ed. L. Bolis, K. Schmidt-Nielsen & S.H.P. Maddrell), pp. 77–97. Amsterdam: North-Holland Publishing Company.

Peters, W. & Pfreundt, C. 1986 Die Verteilung von Trichobothrien und lyraförmigen Organen an den Laufbeinen von Spinnen mit unterschiedlicher Lebensweise. *Zool. Beitr. N. F.* **29**, 209–225.





PHILOSOPHICAL TRANSACTIONS OF THE ROYAL SOCIETY B BIOLOGICAL SCIENCES

Reißland, A. & Görner, P. 1978 Mechanics of trichobothria in orb-weaving spiders (Agelenidae, Araneae). *J. comp. Physiol.* **123**, 59–69.

Reißland, A. & Görner, P. 1985 Trichobothria. In *Neurobiology of arachnids* (ed. F.G. Barth), pp. 138–161. Berlin: Springer-Verlag.

Roeder, K. 1963 Evasive behaviour in the cockroach. In *Nerve cells and insect behaviour*. Cambridge, Massachussets: Harvard University Press.

Seyfarth, E.-A. 1980 Daily patterns of locomotor activity in a wandering spider. *Physiol. Entomol.* **5**, 199–206.

Shimozawa, T. & Kanou, M. 1984 The aerodynamics and sensory physiology of range fractionation in the cercal filiform sensilla of the cricket *Gryllus bimaculatus*. *J. comp. Physiol.* **155**, 495–505.

Stierle, J.E., Getman, M. & Comer, C.M. 1994 Multisensory control of escape in the cockroach *Periplaneta americana*. I. Initial evidence from patterns of wind evoked behaviour. *J. comp. Physiol.* A **174**, 1–11.

Tautz, J. 1977 Reception of medium vibration by thoracal hairs of caterpillars of *Barathra brassicae* L. (Lepidoptera, Noctuidae). I. Mechanical properties of the receptor hairs. *J. comp. Physiol.* **118**, 13–31.

Tautz, J. 1979 Reception of particle oscillation in a medium – an unorthodox sensory capacity. *Naturwissenschaften* **66**, 452–461.

Tautz, J. & Markl, H. 1978 Caterpillars detect flying wasps by hairs sensitive to airborne vibration. *Behav. Ecol. Sociobiol.* **4**, 101–110.

Tobias, M. & Murphey, R.K. 1979 The response of cercal receptors and identified interneurons in the cricket (*Acheta domesticus*) to airstreams. *J. comp. Physiol.* **129**, 51–59.

Treidler, E.B. 1991 An experimental and numerical investigation of flow past ribs in a channel. Ph.D. Thesis, Department of Mechanical Engineering, University of California at Berkeley, Berkeley, California.

Weis-Fogh, T. 1973 Quick estimates of flight fitness in hovering animals, including novel mechanisms for lift production. *J. exp. Biol.* **59**, 169–230.

White, F.M. 1991 *Viscous fluid flow*. New York: McGraw Hill.

Zapfel, K. 1992 Directional characteristics of spider trichobothria. In *Rhythmogenesis in neurons and networks* (ed. N. Elsner & D.W. Richter), p 128. Stuttgart: Thieme-Verlag.

*Received* 1 *September* 1994; *accepted* 18 *October* 1994





PHILOSOPHICAL TRANSACTIONS OF THE ROYAL SOCIETY B BIOLOGICAL SCIENCES

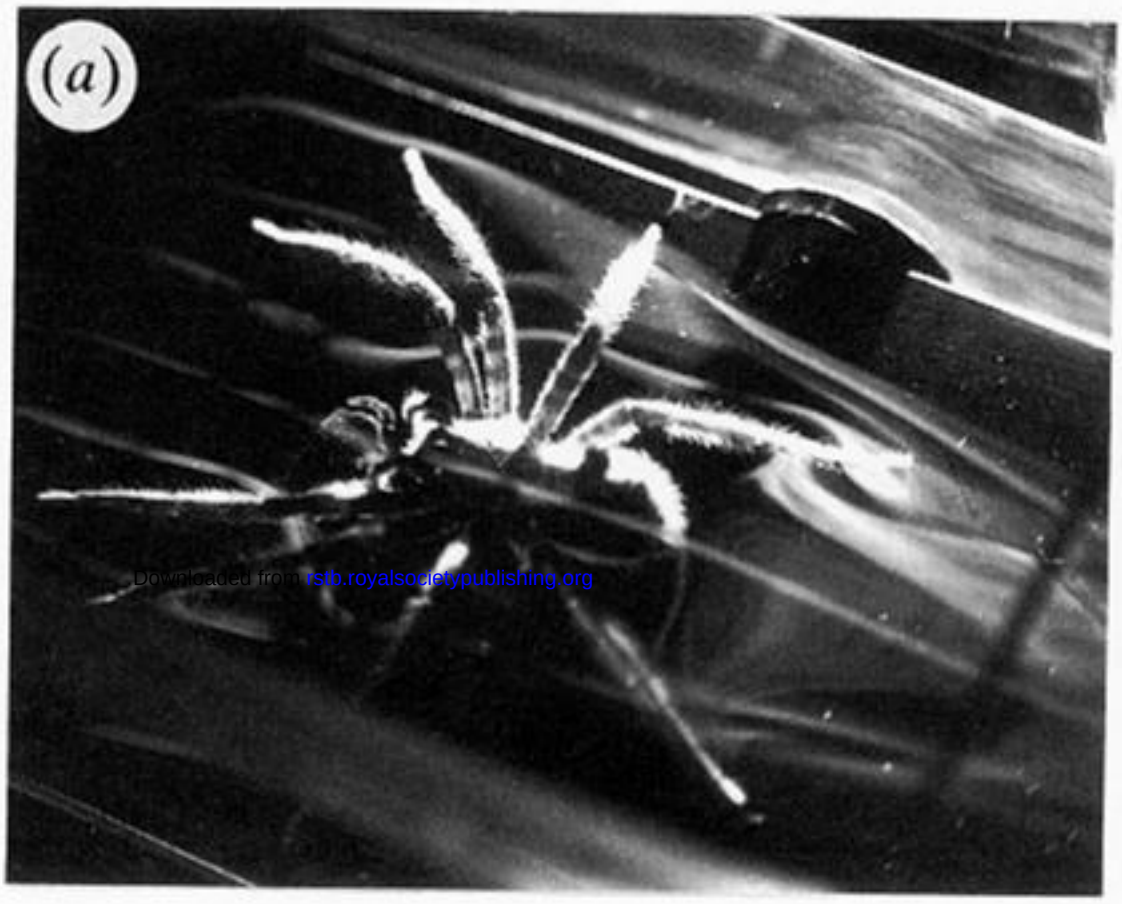




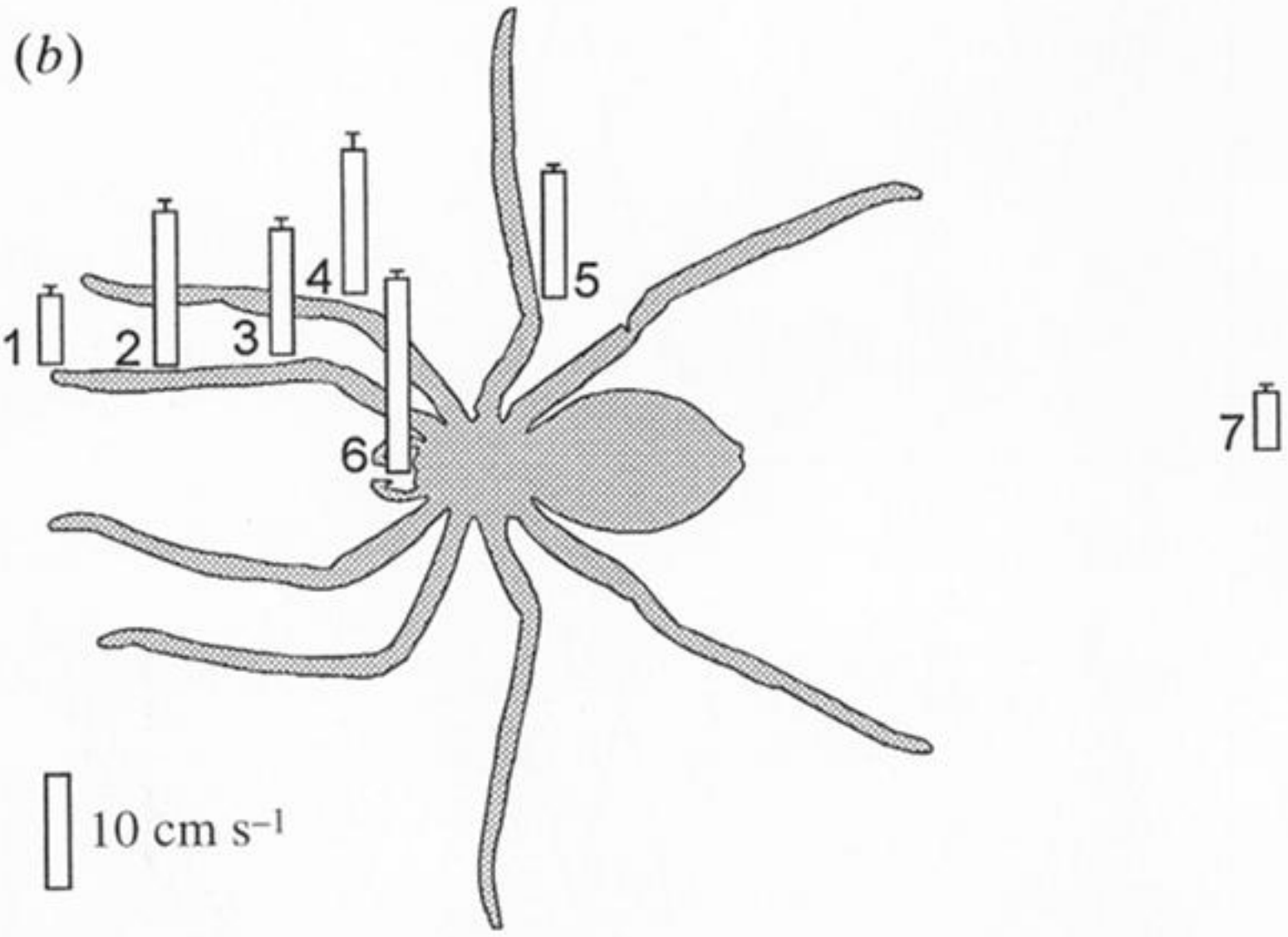


igure 5. Undisturbed air flow around a spider; flow rate $_{\infty}$ = 12 cm s$^{-1}$, spider oriented horizontally and with long xis parallel to air flow. (*a*) Flow visualization reveals an symmetric recirculating flow region in the wake of the pisthosoma and strong curvature of the smoke streaklines in nd around the spaces defined by the spider legs. (*b*) Air peeds measured immediately above different areas of the pider body and behind it. Geometrical arrangement of pider as in (*a*).

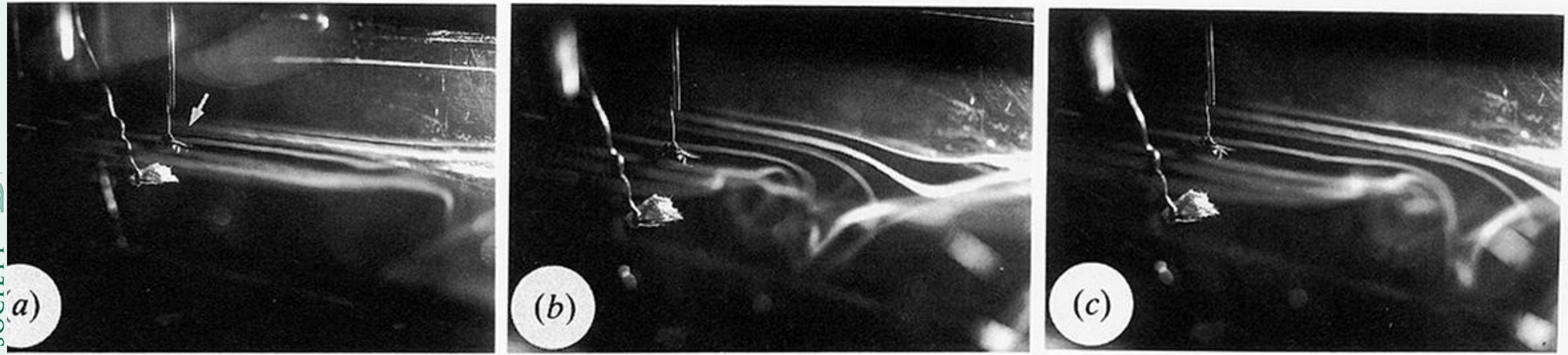


gure 7. Visualization of air flow streaklines produced by stationarily flying fly (arrow). Experiment was performed the wind tunnel shown in figure 1 with $V_0 = 0.12$ m s$^{-1}$. In the photograph sequence the flow is from left to right nd the time interval between photographs is 0.25 s. The streak lines originate at the level of the fly and illustrate e highly vortical and unsteady nature of the fly-generated flow which completely alters the weaker background ow.